Instant Gelation of Various Organic Fluids Including Petrol at Room Temperature by a New Class of Supramolecular Gelators

Darshak R. Trivedi and Parthasarathi Dastidar*

Analytical Science Discipline, Central Salt & Marine Chemicals Research Institute, G. B. Marg, Bhavnagar 364 002, Gujarat, India

Received October 27, 2005. Revised Manuscript Received January 18, 2006

The supramolecular synthon concept has been exploited to generate a series of new organo gelators derived from salts of a primary amine and various derivatives of cinnamic acid. One such gelator, namely, benzylammonium cinnamate **13** (CIN) displays instant gelation ability at room temperature either with or without a brief exposure to sound. Most interestingly, inflammable commercial fluids such as petrol can be gelled instantly by **13** (CIN) at room temperature, which may find real-life applications in containing oil spill, oil mopping, and convenient transport of oil. Analyses of the single-crystal structures of eight salts suggest that structure−property correlation studies in gel research is quite important so that a rational approach may be undertaken to obtain facile synthesis of new gelator compounds.

1. Introduction

Recently, it has been demonstrated by us[1] and others[2] that oils including commercial fuels can be gelled out selectively by gelators from a biphasic mixture of oil/water indicating an alternative method of containing oil spills.[3] However, the heating process involved in a gelation experiment is obviously one of the most serious impediments to be overcome if one has to consider practical or real-life applications of gelators and their gels.

Organic compounds capable of arresting the flow of liquids (gel formation) are popularly known as low molecular mass organic gelators (LMOGs).[4] LMOGs self-assemble into various types of aggregates such as fibers, strands, tapes, and so forth in the gelled state. Such aggregates are shown to cross-link among themselves through "junction zones"[5] to form a three-dimensional (3D) network that immobilizes the solvent molecules and thereby results in gels or viscous liquids. LMOGs have also been found to be used promisingly as structure-directing agents (template) for making helical transition metal oxide[6] and silica,[7] in making microcelluar materials,[8] in the CO_2 based coating process[8] for making dye sensitized solar cells,[9] in biomedical applications[10] and so forth. Therefore, studies on LMOGs have been an active research field in the recent years in materials science and supramolecular chemistry.

However, designing a gelator molecule is still a major challenge and most of the LOMGs reported thus far are either serendipitous or developed from a known gelator molecule. Moreover, making most of such gelators involves time-consuming nontrivial organic syntheses. Thus, facile preparation of compounds as a potential gelator is of utmost importance to find a new and efficient gelling agent.

To design a gelator molecule, it is important to understand the supramolecular architecture (crystal structure) of the metastable gel fiber in its native (gel) form. However, it is virtually impossible to determine the crystal structure of a gel fiber; only an indirect method using X-ray powder diffraction (XRPD) data may be applied.[11] However, recording good quality XRPD data of the gel fibers in its native form generally suffers from the scattering contribution of the solvent molecules and less crystalline nature of the gel fibers, and, therefore, in most of the cases, attempts to record XRPD of gel fibers turn out to be a major disappointment.

On the other hand, correlating single-crystal structure of a molecule in its thermodynamically more stable crystalline state with its gelling/nongelling behavior seems to be more practical. We[12] and others[13] have shown, based on a series

* To whom correspondence should be addressed. Fax: +91-278-2567562. E-mail: parthod123@rediffmail.com; dastidar@csmcri.org.

(1) (a) Trivedi, D. R.; Ballabh, A.; Dastidar, P. *Chem. Mater.* **2003**, *15*, 3971. (b) Trivedi, D. R.; Ballabh, A.; Dastidar, P.; Ganguly, B. *Chem.—Eur. J.* **2004**, *10*, 5311.
(2) Bhattacharya, S.; Krishnan-Ghosh, Y. *Chem. Commun.* **2001**, 185.
(3) Freemantle, M. *Chem. Eng. News* **2001**, *79*, 12.
(4) For excellent reviews on LMOGs, (a) Terech, P.; Weiss, R. G. *Chem. Rev.* **1997**, *97*, 3133. (b) Estroff, L. A.; Hamilton, A. D. *Chem. Rev.* **2004**, *104*, 1201. (c) Grownwald, O.; Shinkai, S. *Curr. Opin. Colloid Interface Sci.* **2002**, *7*, 148. (d) van Esch, J. H.; Ferringa, B. L. *Angew. Chem., Int. Ed.* **2000**, *39*, 2263. (e) Sangeetha, N. M.; Maitra, U. *Chem. Soc. Rev.* **2005**, *34*, 821.
(5) (a) Terech, P.; Ostuni, E.; Weiss, R. G. *J. Phys. Chem.* **1996**, *100*, 3759. (b) Terech, P.; Furman, I.; Weiss, R. G. *J. Phys. Chem.* **1996**, *99*, 9958 and references therein.
(6) Kobayashi, S.; Hamasaki, N.; Suzuki, M.; Kimura, M.; Shirai, H.; Hanabusa, K. *J. Am. Chem. Soc.* **2002**, *124*, 6550.
(7) Jung, J. H.; Ono, Y.; Hanabusa, K.; Shinkai, S. *J. Am. Chem. Soc.* **2000**, *122*, 5008.
(8) Shi, C.; Huang, Z.; Kilic, S.; Xu, J.; Enick, R. M.; Beckmann, E. J.; Carr, A. J.; Melendez, R. E.; Hamilton, A. D. *Science* **1999**, *286*, 1540.
(9) Kubo, W.; Kitamura, T.; Hanabusa, K.; Wada, Y.; Yanagida, S. *Chem. Commun.* **2002**, 374.
(10) (a) Wilder, E. A.; Wilson, K. S.; Quinn, J. B.; Skrtic, D.; Antonucci, J. M. *Chem. Mater.* **2005**, *17*, 2946. (b) Kiyonaka, S.; Sada, K.; Yoshimura, I.; Shinkai, S.; Kato, N.; Hamachi, I. *Nat. Mater.* **2004**, *3*, 58. (c) Kurisawa, M.; Chung, J. E.; Yang, Y. Y.; Gao, S. J.; Uyama, H. *Chem. Commun.* **2005**, 4312. (d) Lee, K. Y.; Mooney, D. J. *Chem. Rev.* **2001**, *101*, 1869. (e) Xing, B.; Yu, C.-W.; Chow, K.-H.; Ho, P.-L; Fu, D.; Xu, B. *J. Am. Chem. Soc.* **2002**, *124*, 14846.
(11) Ostuni, E.; Kamaras, P.; Weiss, R. G. *Angew. Chem., Int. Ed. Engl.* **1996**, *35*, 1324

10.1021/cm0523586 CCC: $33.50
Published on Web 02/16/2006

Scheme 1

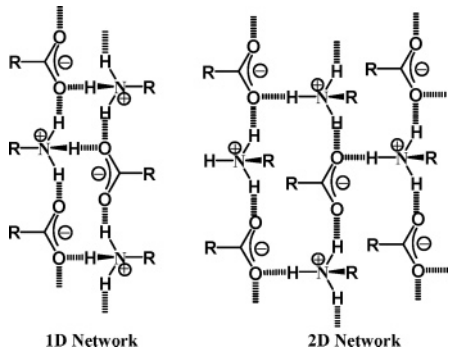

of single-crystal structures, that a one-dimensional (1D) hydrogen bonded network is important for gelation, whereas two-dimensional (2D) and 3D hydrogen bonded networks are not as important. Thus, we decided to work on compounds that might aggregate in a 1D hydrogen bonded network, as potential gelator molecules. Crystal engineering,[14] a powerful technique to gain control over many possible arrangements of molecules to produce solids (crystals) with desired structures and properties, may be employed to generate new, efficient, and easily prepared gelling agents. Out of many approaches to gain control over the arrangement of molecules in space, incorporation of a small number of functional groups that can interact *intermolecularly* through noncovalent interactions (supramolecular synthon[14]) and, therefore, limit the possible arrangements of the molecules in the solid state with respect to one another has been considered one of the most rational approaches. Thus, it is important to identify a suitable supramolecular synthon that might result in aggregation of the molecules in a 1D hydrogen bonded network. We have recently shown that the supramolecular synthon approach is useful in designing a new gelator series.[15]

While searching for a suitable supramolecular synthon that might induce a 1D hydrogen bonded network in the supramolecular assembly, we noticed that primary ammonium monocarboxylate gives a 1D columnar hydrogen bonded network (1D, Scheme 1) in the majority of the cases. It also displays a 2D hydrogen bonded sheet type network (2D, Scheme 1) in a few examples.[16] Thus, we thought it would be worthwhile to study primary ammonium monocarboxylate salts as potential LMOGs because the majority of the crystal structures of such salts may display a 1D hydrogen bonded

Scheme 2

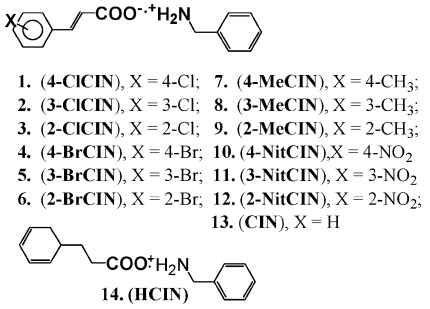

network, which we believe is important for gelation. Thus, we have investigated a series of benzylammonium cinnamate salts as potential gelling agents (Scheme 2).

It may be mentioned here that organic salt based LMOGs are increasingly becoming popular in recent years[17] because the preparation of such salts does not involve time-consuming nontrivial organic syntheses and in a relatively short period of time many salts can be prepared and scanned for their gelation ability. Moreover, the supramolecular self-assembly in such salts is based on strong and directional hydrogen bonding as well as stronger but less directional electrostatic interactions between the cations and the anions.

In this article, we report the syntheses of a series of LMOGs derived from primary ammonium monocarboxylate salts and their gel properties. Few gelators are capable of instant gelation of organic fluids including petrol at room temperature. Structure−property correlation based on single-crystal structures of eight salts in the series (Scheme 2) has also been attempted.

2. Results and Discussion

Gel Formation and Characterization. *Conventional Gelation.* Table 1 lists the gelation data of the salts studied here. In a typical experiment, the gelator is dissolved in a suitable solvent with the aid of few drops of cosolvent (generally MeOH and in the case of salt **11** (3-NitCIN), a 1:1 mixture of MeOH/*N*,*N*-dimethylformamide, DMF) and heating. The solution is then allowed to cool to room temperature under ambient conditions. The container (usually a test tube) is inverted to examine the material's deformity. If no deformation is observed it is termed a gel. It is clear that the majority of the salts studied (8 out of 14 salts) herein shows abilities to harden various organic fluids including commercial fuel such as petrol. The minimum gelator concentration (MGC) and the gel dissociation temperature T_{gel} are within the range of ∼1−6 wt % and 58−108 °C, respectively, indicating significant efficiency and stability of the gels. It is also noticed that no 2-substituted cinnamate salts display any gelation ability with the solvents studied here.

(12) Ballabh, A.; Trivedi, D. R.; Dastidar, P. *Chem. Mater.* **2003**, *15*, 2136 and ref 1.
(13) (a) Luboradzki, R.; Gronwald, O.; Ikeda, M.; Shinkai, S.; Reinhoudt, D. N. *Tetrahedron* **2000**, *56*, 9595. (b) Tamaru, S.-I.; Luboradzki, R.; Shinkai, S. *Chem. Lett.* **2001**, 336.
(14) Desiraju, G. R. *Angew. Chem.* **1995**, *107*, 2541; *Angew. Chem., Int. Ed. Engl.* **1995**, *34*, 2311.
(15) Trivedi, D. R.; Ballabh, A.; Dastidar, P. *J. Mater. Chem.* **2005**, *15*, 2606.
(16) (a) Chenug, E.; Rademacher, K.; Scheffer, J. R.; Trotter, J. *Tetrahedron Lett.* **1999**, *40*, 8733. (b) Kinbara, K.; Kai, A.; Maekawa, Y.; Hashimoto, Y.; Naruse, S.; Hasegawa, M.; Saigo, K. *J. Chem. Soc., Perkin Trans. 2* **1996**, 247. (c) Kinbara, K.; Hashimoto, Y.; Sukegawa, M.; Nohira, H.; Saigo, K. *J. Am. Chem. Soc.* **1996**, *118*, 3441. (d) Kinbara, K.; Tagawa, Y.; Saigo, K. *Tetrahedron: Asymmetry* **2001**, *12*, 2927. (e) Sada, K.; Inoue, K.; Tanaka, T.; Tanaka, A.; Epergyes, A.; Nagahama, S.; Matsumoto, A.; Miyata, M. *J. Am. Chem. Soc.* **2004**, *126*, 1764.
(17) (a) Dastidar, P.; Okabe, S.; Nakano, K.; Iida, K.; Miyata, M.; Tohnai, N.; Shibayama, M. *Chem. Mater.* **2005**, *17*, 741. (b) Nakano, K.; Hishikawa, Y.; Sada, K.; Miyata M.; Hanabusa, K. *Chem. Lett.*, **2000**, 1170. (c) Ayabe, M.; Kishida, T.; Fujita, N.; Sada, K.; Shinkai, S. *Org. Biomol. Chem.* **2003**, *1*, 2744. (d) Oda, R.; Huc I.; Candau, S. J. *Angew. Chem., Int. Ed.* **1998**, *37*, 2689. (e) Abdallah, D. J.; Weiss, R. G. *Chem. Mater.* **2000**, *12*, 406. (f) George, M.; Weiss, R. G. *J. Am. Chem. Soc.* **2001**, *11*, 10393. (g) George, M.; Weiss, R. G. *Langmuir* **2003**, *19*, 1017.

Table 1. Gelation Data (Under Conventional Conditions) of Salts 1, 2, 4, 5, 7, 8, 11, and 13[a]

		1 (4-ClCIN)		**2** (3-ClCIN)		**4** (4-BrCIN)		**5** (3-BrCIN)		**7** (4-MeCIN)		**8** (3-MeCIN)		**11** (3-NitCIN)		13 (CIN)	
series no.	solvent	MGC (wt %)	T_{gel} (°C)	MGC (wt %)	T_{gel} (°C)	MGC (wt %)	T_{gel} (°C)	MGC (wt %)	T_{gel} (°C)	MGC (wt %)	T_{gel} (°C)	MGC (wt %)	T_{gel} (°C)	MGC (wt %)	T_{gel} (°C)	MGC (wt %)	T_{gel} (°C)
1	CCl_4	4.88	82		FC	3.77	70		FC		VL	1.71	86		FC	1.85	68
2	cyclohexane	1.65	68		FC		ppt		ppt	2.38	58		FC		FC	3.27	62
3	*n*-heptane		FC		FC		FC		FC		FC		FC		FC		FC
4	isooctane		FC		FC		FC		ppt		FC		ppt		ppt		FC
5	petrol[a−]		FC	3.62	72	5.84	68		FC		ppt		FC		ppt		FC
6	diesel[a−]		ppt		ppt		ppt		ppt		ppt		ppt		ppt		FC
8	benzene	1.00	78	2.56	77	1.71	69		FC	1.98	74	1.98	63	2.66	70	1.48	63
9	toluene	1.17	86	3.00	82	2.25	98	3.26	80	2.18	88	2.21	84	2.02	79		FC
10	chlorobenzene	2.21	82		VL	2.16	98		ppt	2.17	90	2.13	73	1.98	71		ppt
11	bromobenzene		VL	2.25	84	2.18	100		FC	3.24	90	2.22	68	2.16	77	3.44	60
12	*o*-xylene	1.93	80	2.21	71	1.95	105		FC	1.90	94	2.06	74	1.85	82		FC
13	*m*-xylene	1.57	91	2.14	80	2.14	103	2.33	76	2.13	71	2.13	82	1.88	84		FC
14	*p*-xylene	2.30	102	2.33	83	2.16	104		FC	2.16	88		VL	1.96	80	2.60	72
15	mesitylene	2.12	81		VL	2.23	108		ppt		VL	2.93	88		ppt		FC
16	1,2-dichloro-benzene		VL		FC	2.22	101		FC	2.05	71	2.12	86	1.65	80	2.17	65
17	dimethyl formamide		ppt		ppt				ppt		ppt		ppt		S		ppt
18	nitrobenzene	2.25	63		VL	2.54	96		ppt		VL		VL	1.61	78		FC
19	methyl salicylate		ppt		VL	2.14	102		S	2.09	90		FC	1.93	66	2.18	66
20	ethyl acetate		FC		FC	3.13	82		ppt		FC		FC	2.56	65		FC
21	dimethyl-sulfoxide		S		S	−	S		S		S		S		S		S

wt % = g/100 mL of solvent. [a] g/100 g of solvent. FC = fibrous crystals. ppt = precipitate. S = solution. VL = viscous liquid.

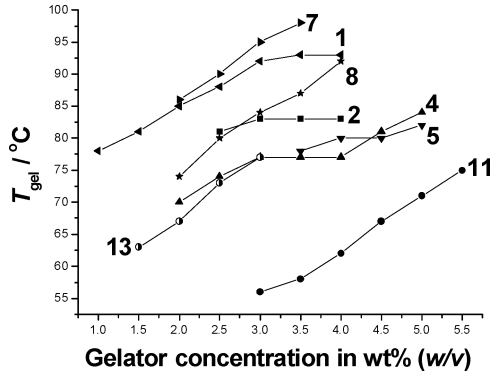

Figure 1. T_{gel} vs gelator concentration plots. The numbers on the plots indicate the gelator numbers. While **5** (3-BrCIN) and **11** (3-NitCIN) represent tolune gel, the rest of the plots represent benzene gel.

Steady increase of T_{gel} as a function of gelator concentration in all the gelators indicates that the self-assembly in the gel state is driven by strong intermolecular interactions (Figure 1).

Instant Gelation. All the gelators are tested for instant gelation except salts **1** (4-ClCIN), **4** (4-BrCIN), **10** (4-NitCIN), **11** (3-NitCIN), and **12** (2-NitCIN) because of the solubility problem of the acid part of the salts. Salt **13** (CIN) is studied in detail with various solvents for instant gelation because cinnamic acid is a low cost material compared to the other acid derivatives used in this study. Table 2 lists the details of the instant gelation of the solvents studied here. In a typical experiment, the acid is dissolved in the suitable solvent (to be gelled) with the help of a few drops of MeOH (if required) followed by sonication (if required). To this mixture is added a stoichiometric amount of benzylamine, and it is immediately sonicated (0.04 W/cm^3, 42.0 kHz) for 3−4 s (if required). The gel is formed instantaneously in most of the cases (Table 2).

Table 2. Instant Gelation Data for Salt 13[a]

series no.	solvent for gelation	cosolvent (few drops)	sonication time (s)	time taken for gelation	wt % (in w/v)
1	petrol (3 mL)	MeOH	3−4	instant	8.5
2	benzene (3 mL)			instant	8.5
3	toluene (3 mL)	MeOH		instant	8.5
4	cyclohexane (6 mL)	MeOH	3−4	2 h	4.2
5	CCl_4 (6 mL)	MeOH	3−4	instant	4.2
6	Br−benzene (6 mL)		3−4	instant	4.2
7	*p*-xylene (4 mL)	MeOH		instant	6.3
8	methylsalicylate (3 mL)		3−4	instant	8.5
9	CH_3CN (6 mL)			instant	4.2

[a] The final amount of the salt is 1 mmol.

It is remarkable to note that salt **13** (CIN) is able to gel nine organic solvents instantaneously at room temperature; an external stimulus such as ultrasound is required in some cases. In all the cases, the gels are thermoreversible except in the case of petrol gel. It is also interesting to note that salt **13** (CIN) is unable to gel petrol in a conventional manner (Table 1). Besides salt **13** (CIN), salts **2** (3-ClCIN), **5** (3-BrCIN), **8** (3-MeCIN), and **14** (HCIN) display the ability of instant gelation of ethyl acetate (3 mL) when 0.5 mmol of reactants is used. Sonication (0.04 W/cm^3, 42.0 kHz) for 3−4 s is required for **2** (3-ClCIN) and **14** (HCIN) whereas **5** (3-BrCIN) and **8** (3-MeCIN) gave instant gelation without sonication. While there are few reports[18] on instant gelation of organic fluids in isothermal conditions (room temperature), there are no reports wherein a commercial fuel (such as petrol) has been gelled instantaneously at room temperature. The ability of salt **13** (CIN) to gel petrol instantly is,

(18) (a) George, M.; Weiss, R. G. *Langmuir* **2003**, *19*, 1017. (b) Suzuki, M.; Nakajima, Y.; Yumoto, M.; Kimura, M.; Shirai, H.; Hanabusa, K. *Org. Biomol. Chem.* **2004**, *2*, 1155.

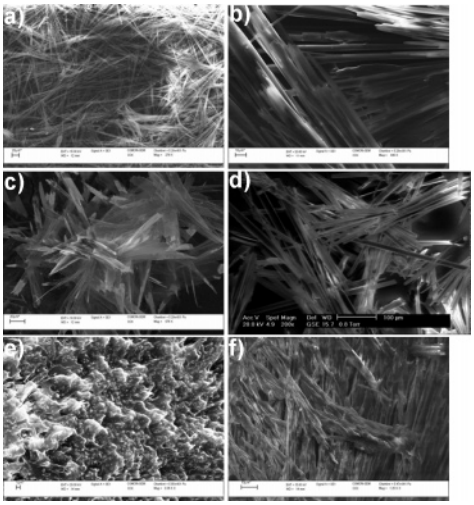

Figure 2. SEM micrographs of xerogels (a) **1** (4-ClCIN) in benzene (2.5 wt %, conventional, bar = 20 μm; (b) **2** (3-ClCIN) in petrol (4.0 wt %, conventional, bar = 10 μm; (c) **13** (CIN) in petrol (8.5 wt %, instant, bar = 20 μm); (d) **13** (CIN) in toluene (4.2 wt %, instant, bar = 100 μm); (e) **13** (CIN) in benzene (2.5 wt %, conventional, bar = 1 μm); and (f) **13** (CIN) in benzene, instant, bar = 10 μm).

therefore, very important in realistic applications such as in containing an oil spill, oil mopping, and so forth. However, the same experiment (instant gelation) with a biphasic mixture of petrol/water turn out to be a failure presumably because of high solubility of the resulting salt **13** (CIN) in water. It may be noted that sound induced gelation is also a rare phenomenon, and to the best of our knowledge, there is only one such report of this in the literature.[19]

Scanning electron microscopy (SEM) micrographs are recorded for xerogels derived from a few gelators (Figure 2) to see the detail of the gel fiber morphology. In the cases studied, a typical 3D network of fibers in the xerogels is observed both in conventional and in instant gelation conditions (Figure 2a−d). However, it is interesting to note that salt **13** (CIN) displays different morphologies of the xerogels derived from same solvent benzene under conventional and instant gelation conditions. The solvent molecules are understandably immobilized in such a network of fibers in the gel state.

Structure−Property Correlation. To establish a starting hypothesis based on which potential gelator molecules may be synthesized, it is important to study the single-crystal structures of both gelators and nongelators, and the corresponding property (gelation/nongelation). In fact, the present study is based on a rational approach that primary ammonium monocarboxylate salts should display a 1D hydrogen bonded network (Scheme 1) and, therefore, may be considered as potential gelators. It is significant that out of the 14 salts prepared, 8 salts are gelators. Efforts to crystallize all the salts reported herein result in X-ray quality single crystals of gelators **2** (3-ClCIN), **5** (3-BrCIN), **7** (4-MeCIN), **8** (3-MeCIN), **11** (3-NitCIN), and **13** (CIN) and nongelators **6** (2-BrCIN) and **9** (2-MeCIN), which are subjected to XRPD measurements.

Single-Crystal Structures of Gelator Salts. *Crystal Structure of Benzylammonium-3-chlorocinnamate **2**.* Salt **2** (3-ClCIN) belongs to the centrosymmetric monoclinic space group $P2_1/c$. The asymmetric unit contains an ion pair. In the crystal structure, three ammonium protons are holding three symmetry related 3-chlorocinnamate anions by strong N−H···O hydrogen bonding (N···O = 2.756(3)−2.802(3) Å; ∠N−H···O = 151.0(2)−173.0(3)°). Such hydrogen bonding interactions lead to the formation of a staircase-like 1D hydrogen bonded network (Figure 3).

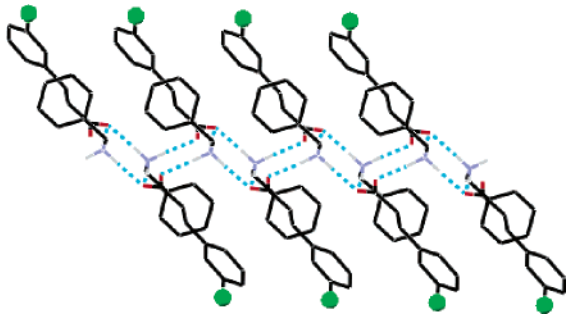

Figure 3. 1D columnar staircase-like hydrogen bonded network observed in the crystal structure of gelator salt **2** (3-ClCIN).

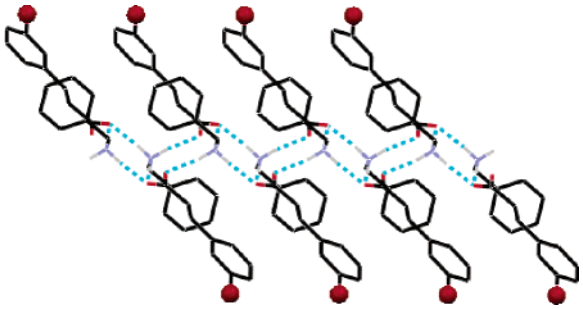

Figure 4. 1D columnar staircase-like hydrogen bonded network observed in the crystal structure of gelator salt **5** (3-BrCIN).

Secondary interactions such as C−H···π involving both the aromatic moieties of the cation and the aromatic moieties of the anion appear to play a significant role in stabilizing the 1D network further ($H_{aromatic/anion}\cdots\pi_{centroid/cation}$ = 3.208 Å; $H_{aromatic/cation}\cdots\pi_{centroid/anion}$ = 2.910 Å; $\angle C-H_{aromatic/anion}\cdots\pi_{centroid/cation}$ = 135.5°, $\angle C-H_{aromatic/cation}\cdots\pi_{centroid/anion}$ = 130.2°).

*Crystal Structure of Benzylammonium-3-bromocinnamate **5**.* The asymmetric unit in the crystal structure of **5** (**3-BrCIN**) (monoclinic $P2_1/c$) is comprised of one ion pair. The cationic protons hold three symmetry related anionic moieties through N−H···O hydrogen bonding (N···O = 2.760(4)−2.801(5) Å; ∠N−H···O = 149.0(4)−170.0(4)°) resulting in a staircase-like 1D hydrogen bonded network (Figure 4).

While secondary interactions such as C−H···π involving both the aromatic moieties of the cation and the aromatic moieties of the anion appear to play a significant role in stabilizing the 1D network further ($H_{aromatic/anion}\cdots\pi_{centroid/cation}$ = 3.224 Å; $H_{aromatic/cation}\cdots\pi_{centroid/anion}$ = 2.906 Å; $\angle C-H_{aromatic/anion}\cdots\pi_{centroid/cation}$ = 135.5°, $\angle C-H_{aromatic/cation}\cdots\pi_{centroid/anion}$ = 130.4°), inter-network C−H···Br interactions (C···Br = 3.779 Å; ∠C−H···Br = 137.6°) seem to stabilize the overall crystal structure.

*Crystal Structure of Benzylammonium-4-methylcinnamate **7**.* Salt **7** (4-MeCIN) crystallizes in the centrosymmetric monoclinic space group $P2_1/c$. The asymmetric unit contains

(19) Naota, T.; Koori, H. *J. Am. Chem. Soc.* **2005**, *127*, 9324.

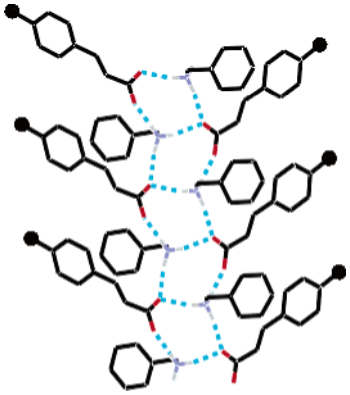

Figure 5. 1D columnar hydrogen bonded network observed in the crystal structure of gelator salt **7** (4-MeCIN).

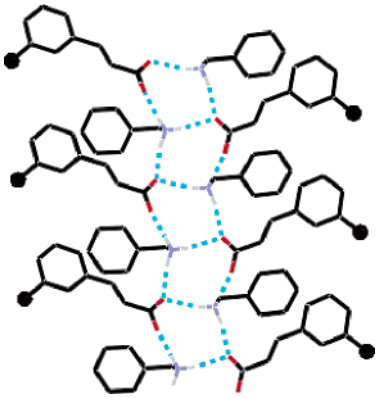

Figure 6. 1D columnar hydrogen bonded network observed in the crystal structure of gelator salt **8** (3-MeCIN).

one ion pair. Three symmetry related anionic species are held together by three protons of one cationic moiety through N−H···O hydrogen bonding interactions (N···O = 2.609(3)−2.769(3) Å; ∠N−H···O = 153.0(3)−175.0(3)°), which lead to the formation of a corrugated 1D hydrogen bonded network of ions (Figure 5). The 1D networks are further packed in the crystal lattice via van der Waals interactions.

*Crystal Structure of Benzylammonium-3-methylcinnamate **8***. The crystal of salt **8** (3-MeCIN) belongs to the monoclinic $P2_1/c$ space group, and the asymmetric unit contains one ion pair. Through various N−H···O interactions (N···O = 2.724(3)−2.765(3) Å; ∠N−H···O = 158.0(3)−177.0(3)°), each cation is holding three symmetry related anionic moieties resulting in a corrugated 1D hydrogen bonded network (Figure 6). The 1D networks are packed in the crystal structure in a parallel fashion further stabilized by C−H···π interactions involving the aromatic ring of the cation of one 1D network and methylene group of the cation coming from a neighboring 1D network ($H\cdots\pi_{centroid/cation}$ = 2.803 Å; ∠C−H···$\pi_{centroid/cation}$ = 121.9°) and dispersion forces.

*Crystal Structure of Benzylammonium-3-nitrocinnamate **11***. Salt **11** (3-NitCIN) crystallizes in a noncentrosymmetric orthorhombic space group $P2_12_12_1$, and its asymmetric unit contains one ion pair. The three protons of ammonium cation hold three symmetry related anions through N−H···O hydrogen bonding (N···O = 2.717(3)−2.781(3) Å; ∠N−H···O = 168.0(3)−172.0(3)°) resulting in a corrugated 1D hydrogen bonded network (Figure 7). The 1D networks

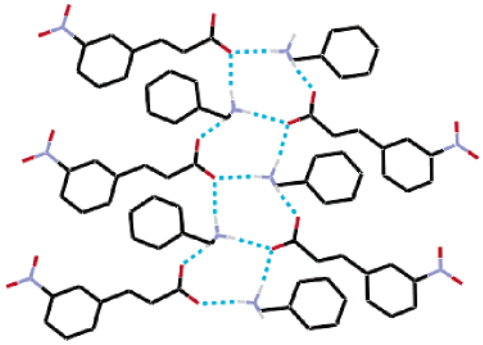

Figure 7. 1D columnar hydrogen bonded network observed in the crystal structure of gelator salt **11** (3-NitCIN).

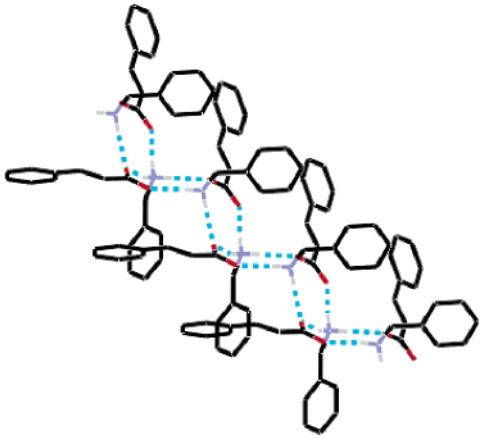

Figure 8. 1D columnar staircase-like hydrogen bonded network observed in the crystal structure of gelator salt **13** (CIN).

are packed in the crystal lattice in a parallel fashion, further stabilized by C−H···O interactions (C···O = 3.382 Å; ∠C−H···O = 145.3°) involving the methylene proton of the cation and oxygen of nitogroup of the anion.

*Crystal Structure of Benzylammonium Cinnamate **13***. The crystal of salt **13** (CIN) belongs to a noncentrosymmetric orthorhombic space group $P2_12_12_1$, and the asymmetric unit contains one ion pair. Three symmetry related anionic moieties are held together by one cationic species via N−H···O hydrogen bonding (N···O = 2.703(2)−2.749(2); ∠N−H···O = 162.9(2)−176.0(2)°) resulting in a staircase-like 1D hydrogen bonding network (Figure 8). The 1D networks are packed in the crystal lattice in a parallel fashion further sustained by C−H···π interactions involving the aromatic C−H proton of the anion and ethylene moiety of the anion coming from neighboring network ($H_{aromatic/anion}\cdots\pi_{centroid/ethylene\ moiety/anion}$ = 2.889 Å; ∠C−H···π = 156.6°) and dispersion forces.

Single-Crystal Structures of Nongelator Salts. *Crystal Structure of Benzylammonium-2-bromocinnamate **6***. Salt **6** (2-BrCIN) crystallizes in a centrosymmetric triclinic space group $P\bar{1}$, and its asymmetric unit contains two ion pairs and two solvate water molecules. Ammonium cations are holding three symmetry related anions through N−H···O hydrogen bonding (N···O = 2.762(7)−2.857(6); ∠N−H···O = 161.0(4)−180.0(6)°). These interactions lead to the formation of a staircase-like 1D hydrogen bonded network. The solvate water molecules form a 1D infinite hydrogen bonded chain (O···O = 2.778−2.909 Å), and such chains of solvate water molecules act as a linker among the

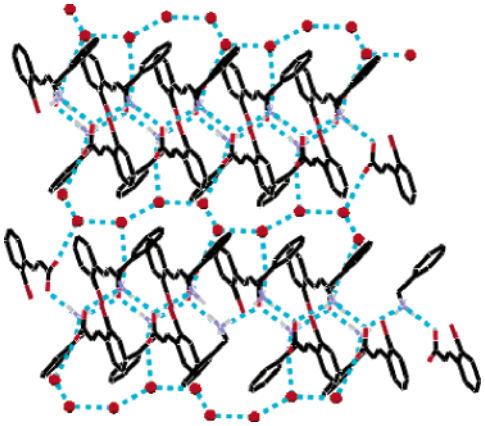

Figure 9. Staircase-like 1D hydrogen bonded networks connected by an infinite water chain in salt **6** (2-BrCIN).

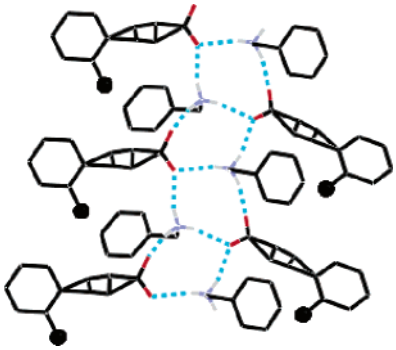

Figure 10. 1D hydrogen bonded network in salt **9** (2-MeCIN). The ethylene backbone is disordered.

1D hydrogen bonded network of ion pairs resulting in an overall 2D hydrogen bonded network (Figure 9).

Crystal Structure of Benzylammonium-2-methylcinnamate ***9***. Salt **9** (2-MeCIN) belongs to centrosymmetric monoclinic space group $P2_1/c$, and the asymmetric unit contains one ion pair. The unsaturated backbone of the anionic moiety is found to be disordered. The 1D corrugated hydrogen bonded network involving cations and anions via N−H···O type hydrogen bonding (N···O = 2.687(5)−2.789(4); ∠N−H···O = 161.0(4)−164.0(4)°) is observed (Figure 10). In the crystal lattice, various secondary interactions such as C−H···O (C···O = 3.262 Å; ∠C−H···O = 150.4°) involving anionic oxygen and the aromatic C−H proton of the cation and C−H···π involving the cationic aromatic proton and π cloud of the unsaturated backbone of the anion ($H_{aromatic/cation}\cdots\pi_{centroid/ethylene\ \ moiety/anion}$ = 3.020 Å; ∠C−H···π = 146.8°) and the methyl proton of anion and π cloud of the aromatic ring of the cation (H···π = 2.903 Å; ∠C−H···π = 138.4°) are observed.

Thus, all the crystal structures studied herein display 1D columnar hydrogen bonded network as envisaged (Scheme 1). However, careful analyses of these structures reveal that there are three types of supramolecular connectivities within the 1D columnar network (Figure 11). Salts **2** (3-ClCIN) and **5** (3-BrCIN) display identical supramolecular hydrogen bonded networks. Alternating 8- and 12-membered rings of hydrogen bonded ion pairs are observed in these salts. In 8-membered rings, both the oxygen atoms display bifurcated hydrogen bonding interactions with the cations within the ring, whereas in 12-membered rings, oxygen atoms show

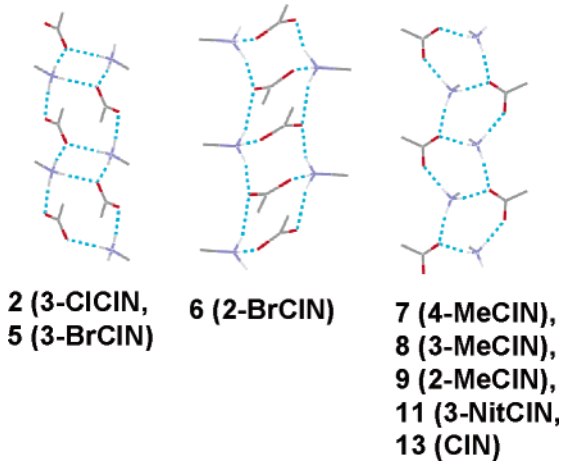

Figure 11. Various supramolecular connectivities within the 1D hydrogen bonded network in the crystal structures of the salts studied.

usual hydrogen bonding interactions with the cationic protons within the ring.

On the other hand, salt **6** displays a different supramolecular connectivity wherein the 12-membered hydrogen bonded rings of the ion pair are observed within the network. The oxygen atoms within the ring display the usual hydrogen bonding interactions with the cations. Interestingly, salts **7**−**9**, **11**, and **13** show identical supramolecular connectivity. In these cases, 10-membered hydrogen bonded rings of cations and anions are present within the 1D-columnar network. Only one oxygen atom within the ring forms bifurcated hydrogen bonding interactions with the cationic protons.

Thus, it is clear from the crystallographic data that all the gelator salts **2**, **5**, **7**, **8**, **11**, and **13** display a 1D columnar hydrogen bonded network despite having different supramolecular connectivities within the network. The results correspond well with the fact that the 1D hydrogen bonded network tends to show gelation ability.[12,13] However, salts **6** and **9** are not capable of hardening any solvents studied herein despite having a 1D columnar hydrogen bonded network. It is quite reasonable to believe that a 1D hydrogen bonded network may be one of the prerequisites for a molecule to show gelation ability; complicated and not yet understood interactions between the gel fibers and solvent molecules play significant roles in immobilizing the solvents within the fibrous network of the gelator.

Gel formation may be considered as a kind of crystallization phenomenon because the fibers in the native (gel) as well as in the xerogel (dried gel) state often diffract X-rays. The crystalline phase (morph) responsible for gel formation might not be the thermodynamically most stable one, and, therefore, such a phase transformation is quite possible while removing the solvent during xerogel formation. There is no certainty that such a change does occur during xerogel formation, but there is no evidence that it does not. Thus, it is important to compare XRPDs of the bulk solid with that of the xerogel and gel fibers. In the present study, no meaningful diffraction was observed for the gel state of any of the gelators presumably because of the severe scattering coming from solvent molecules. However, the corresponding xerogels gave reasonable diffraction. Except for **13** (CIN), all the gelators show reasonable correspondence with the

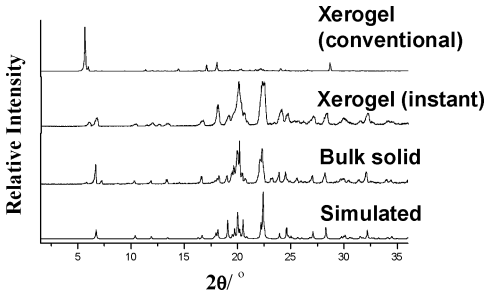

Figure 12. XRPDs of salt **13** (CIN) under various conditions.

XRPDs of bulk solid with the corresponding XRPDs of xerogels derived from various solvents, meaning that the molecular packing of the gelator in the crystal (bulk solid) resembles that present in the fibers of the xerogels (Figure S1, Supporting Information).

On the other hand, XRPDs of xerogels of **13** (CIN) prepared under various conditions (from benzene solvent; both under conventional and instant gelation methods) display different patterns (Figure 12). While the XRPD of the xerogel prepared under the instant gelation condition shows good agreement with that of bulk solid and simulated pattern obtained from single-crystal data, the XRPD of the xerogel obtained from conventional gelation method does not match with that obtained from the bulk solid and simulated pattern. This means that the molecular packing in the fibers of the xerogel (instant) resembles well with that of in the bulk solid, whereas it is not true in the case of the fibers in the xerogel (conventional). In this context, it is interesting to note that the fiber morphologies of the benzene xerogel of **13** (CIN) prepared under conventional and instant gelation conditions are also different (Figure 2). Good agreement between the simulated XRPD and the bulk solid XRPD in all the salts for which crystal structures are determined indicate significant crystalline phase purity during the synthesis of the salts (Figures S1 and S2, Supporting Information). It may be noted that the xerogel fibers of **1**, **2**, **4**, **5**, **7**, **8**, and **11** represent the same crystalline phase of the bulk solid and single-crystal form (except for **1** and **4** for which single-crystal data could not be obtained; Figure S1, Supporting Information).

3. Conclusions

Thus, we have successfully demonstrated the aptitude of supramolecular synthon concepts in designing new LMOGs. On the basis of the well-established supramolecular synthons, a series of salts (Scheme 2) have been prepared, and delightfully, the majority of the salts (**1**, **2**, **4**, **5**, **7**, **8**, **11**, and **13**) shows excellent gelation abilities. Ability of the gelator **13** (CIN) to harden instantaneously (in most cases) various organic liquids including commercial fuel such as petrol at room temperature is quite noteworthy and may be useful in fabricating a real-life application in containing solvent/oil spills, mopping, and safe transport of inflammable fluids.

Single-crystal structures of the salts reported herein display a 1D columnar hydrogen bonded network irrespective of their properties (gelation/nongelation). However, the majority of the gelator salts subjected to single-crystal XRPD shows a 1D hydrogen bonded network indicating a remarkable structure−property correlation. The fact that nongelator salts **6** and **9** also display 1D network demands further understanding of the interactions between gel fibers and solvent molecules. The facile syntheses of the series of organo gelators exploiting the concept of noncovalent synthesis (supramolecular synthon approach) presented here should contribute significantly toward the development of the design and facile synthesis of organic soft materials.

4. Experimental Section

Materials and Physical Measurements. All chemicals (Aldrich) and the solvents used for gelation (A.R. grade, S.D. Fine Chemicals, India) are used without further purification. All the oils are procured from the local market. Microanalyses are performed on a Perkin-Elmer elemental analyzer 2400, series II. Fourier transform infrared (FT-IR) and ^{1}H NMR spectra are recorded using Perkin-Elmer Spectrum GX and 200 MHz Bruker Avance DPX200 spectrometers, respectively. XRPD patterns are recorded on an XPERT Philips (Cu Kα radiation) diffractometer. SEM is performed on a LEO 1430VP.

Syntheses. *Salts **1** and **4**.* A solution of corresponding acid (1.0 mmol) in hot nitrobenzene was prepared with the aid of a few drops of MeOH. To this solution was added slowly benzylamine (1.0 mmol), and the reaction mixture was kept at room temperature. After a few hours, the whole reaction mixture was found to be gelled. Acetonitrile was then added to the gel to destroy the gel network, and the salts **1** and **4** as a white precipitate were then isolated by filtration (near quantitative yield) and used for gelation and other studies.

*Salts **10**−**12**.* A solution of corresponding acid (1.0 mmol) in hot DMF was prepared with the aid of a few drops of MeOH. To this solution was added slowly benzylamine (1.0 mmol), and the reaction mixture was kept at room temperature. After a few hours, the resulting salts as precipitates (near quantitative yield) were used for gelation and other studies.

*Salts **2**, **3**, **5**−**9**, **13**, and **14**.* The corresponding acid (1 mmol) was dissolved in MeOH by sonication. Benzylamine (1.0 mmol) was added slowly to the methanolic solution of the acid at room temperature. The reaction mixture was then allowed to evaporate to dryness at room temperature. The resulting salts as precipitates (near quantitative yield) were used for gelation and other studies.

Analytical Data. ***1** (4-ClCIN).* 168 °C. Anal. Calcd for $C_{16}H_{16}NO_2Cl$: C, 66.32; H, 5.57; N, 4.83. Found: C, 66.16; H, 6.77; N, 4.88. ^{1}H NMR (200 MHz, CD_3OD): δ = 7.32−7.52 (10H, m); 6.45−6.53 (1H, d); 4.09 (2H, s). FT-IR (KBr): 3469, 3037, 3011, 2975, 2947, 2883, 2547, 2472, 2361, 2094, 1915, 1827, 1780, 1641, 1589, 1526, 1490, 1456, 1406, 1369, 1284, 1249, 1195, 1161, 1111, 1087, 1011, 980, 963, 929, 882, 841, 827, 786, 732, 699, 662, 634, 619, 577, 532, 499, 451, 417 cm^{-1}.

***2** (3-ClCIN).* Mp 118 °C. Anal. Calcd for $C_{16}H_{16}NO_2Cl$: C, 66.32; H, 5.57; N, 4.83. Found: C, 65.92; H, 5.57; N, 4.72. ^{1}H NMR (200 MHz, CD_3OD): δ = 7.29−7.52 (10H, m); 6.47−6.55 (1H, d); 4.10 (2H, s). FT-IR (KBr): 3471, 3066, 2833, 2600, 2362, 2145, 1772, 1633, 1564, 1533, 1482, 1456, 1416, 1383, 1370, 1309, 1254, 1213, 1198, 1150, 1097, 1079, 981, 922, 905, 876, 852, 793, 750, 699, 684, 674, 589, 534, 482, 437 cm^{-1}.

***3** (2-ClCIN).* Mp 115 °C. ^{1}H NMR (200 MHz, CD_3OD): δ = 7.70−7.95 (3H, m); 7.29−7.43 (7H, m); 6.47−6.55 (1H, d); 4.11 (2H, s). FT-IR (KBr): 3394, 3293, 3057, 2989, 2874, 2646, 2363, 2186, 1686, 1637, 1580, 1513, 1501, 1470, 1441, 1387, 1340, 1305, 1284, 1226, 1204, 1160, 1121, 1073, 1037, 1009, 971, 934, 878, 767, 752, 735, 694, 676, 595, 577, 461, 443, 408 cm^{-1}.

Table 3. Crystallographic Parameters for Salts 2, 5, 6−9, 11, and 13

crystal data	**2** (3-ClCIN)	**5** (3-BrCIN)	**6** (2-BrCIN)	**7** (4-MeCIN)
empirical formula	$C_{16}H_{16}ClNO_2$	$C_{16}H_{16}BrNO_2$	$C_{32}H_{33}Br_2\ N_2\ O_6$	$C_{17}H_{19}\ NO_2$
fw	289.75	334.21	701.42	269.33
crystal size (mm), color	0.33 × 0.47 × 0.18 colorless	0.45 × 0.71 × 0.38 colorless	0.56 × 0.34 × 0.28 colorless	0.57 × 0.36 × 0.49 colorless
crystal system	monoclinic	monoclinic	triclinic	monoclinic
space group	$P2_1/C$	$P2_1/C$	$P\bar{1}$	$P2_1/C$
a (Å)	5.6986(7)	5.7055(6)	9.344(2)	15.5079(19)
b (Å)	31.167(4)	31.500(3)	12.598(3)	6.3639(8)
c (Å)	8.4559(10)	8.4935(9)	13.973(3)	16.653(2)
α (deg)	90.00	90.00	79.155(4)	90.00
β (deg)	101.863(2)	102.029(2)	85.812(4)	112.019(2)
γ (deg)	90.00	90.00	83.454(5)	90.00
volume (Å^3)	1469.8(3)	1492.9(3)	1602.7(7)	1523.6(3)
Z	4	4	2	4
D_{calcd}	1.309	1.487	1.453	1.174
F(000)	608	680	714	576
μ(Mo Kα) (mm^{-1})	0.260	2.754	2.573	0.077
temperature (K)	293(2)	293(2)	293(2)	293(2)
observed reflections [$I > 2\sigma(I)$]	1636	1557	2727	1620
parameters refined	193	193	407	246
goodness of fit	1.059	1.032	1.027	1.084
final R_1 on observed data	0.0372	0.0389	0.0518	0.0572
final wR_2 on observed data	0.0869	0.0837	0.1226	0.1566

crystal data	**8** (3-MeCIN)	**9** (2-MeCIN)	**11** (3-NitCIN)	**13** (CIN)
empirical formula	$C_{17}H_{19}NO_2$	$C_{17}H_{17}N\ O_2$	$C_{16}H_{16}N_2\ O_4$	$C_{16}H_{17}NO_2$
fw	269.33	267.32	300.31	255.31
crystal size (mm), color	0.63 × 0.46 × 0.48 colorless	0.68 × 0.39 × 0.26 colorless	0.39 × 0.62 × 0.45 light yellow	0.52 × 0.38 × 0.28 colorless
crystal system	monoclinic	monoclinic	orthorhombic	orthorhombic
space group	$P2_1/C$	$P2_1/C$	$P2_12_12_1$	$P2_12_12_1$
a (Å)	15.132(2)	14.7304(14)	6.0436(5)	5.9610(7)
b (Å)	6.4059(10)	6.4104(6)	12.4857(11)	8.9939(10)
c (Å)	15.489(2)	15.4761(15)	20.7079(19)	26.337(3)
α (deg)	90.00	90.00	90.00	90.00
β (deg)	93.516(3)	91.706(2)	90.00	90.00
γ (deg)	90.00	90.00	90.00	90.00
volume (Å^3)	1498.6(4)	1460.7(2)	1562.6(2)	1412.0(3)
Z	4	4	4	4
D_{calcd}	1.194	1.216	1.277	1.201
F(000)	576	568	632	544
μ(Mo Kα) (mm^{-1})	0.078	0.080	0.093	0.079
temperature (K)	293(2)	293(2)	293(2)	293(2)
observed reflections [$I > 2\sigma(I)$]	1734	1721	1804	1784
parameters refined	194	192	211	184
goodness of fit	1.054	1.064	1.107	1.093
final R_1 on observed data	0.0592	0.0849	0.0400	0.0347
final wR_2 on observed data	0.1536	0.2332	0.0869	0.0849

4 *(4-BrCIN).* Mp 180 °C. Anal. Calcd for $C_{16}H_{16}NO_2Br$: C, 57.50; H, 4.83; N, 4.19. Found: C, 57.40; H, 5.08; N, 3.75. ^{1}H NMR (200 MHz, CD_3OD): δ = 7.30−7.53 (10H, m); 6.46−6.54 (1H, d); 4.09 (2H, s). FT-IR (KBr): 3122, 3059, 3043, 3010, 2946, 2475, 2089, 1914, 1640, 1581, 1524, 1486, 1402, 1380, 1352, 1282, 1250, 1196, 1160, 1109, 1072, 1007, 980, 962, 928, 881, 840, 825, 728, 698, 634, 577, 531, 494, 465, 420 cm^{-1}.

5 *(3-BrCIN).* Mp 120 °C. Anal. Calcd for $C_{16}H_{16}NO_2Br$: C, 57.50; H, 4.83; N, 4.19. Found: C, 57.22; H, 5.03; N, 3.79. ^{1}H NMR (200 MHz, CD_3OD): δ = 7.23−7.67 (10H, m); 6.45−6.54 (1H, d); 4.10 (2H, s). FT-IR (KBr): 3062, 3031, 3017, 2828, 2596, 2142, 1958, 1890, 1769, 1692, 1634, 1563, 1532, 1478, 1456, 1415, 1371, 1307, 1253, 1212, 1196, 1148, 1115, 1071, 980, 923, 907, 874, 789, 748, 730, 698, 668, 587, 533, 481, 431 cm^{-1}.

6 *(2-BrCIN).* Mp 72 °C. Anal. Calcd for $C_{16}H_{16}NO_2Br$: C, 57.50; H, 4.83; N, 4.19. Found: C, 57.22; H, 5.03; N, 3.79. ^{1}H NMR (200 MHz, CD_3OD): δ = 7.20−7.82 (10H, m); 6.42−6.50 (1H, d); 4.10 (2H, s). FT-IR (KBr): 3391, 3287, 3054, 2988, 2870, 2755, 2645, 2183, 1965, 1883, 1819, 1638, 1579, 1511, 1501, 1466, 1437, 1387, 1283, 1201, 1162, 1144, 1072, 1022, 969, 933, 879, 857, 849, 766, 736, 693, 656, 591, 577, 545, 506, 460, 439 cm^{-1}.

7 *(4-MeCIN).* Mp 174 °C. Anal. Calcd for $C_{17}H_{19}NO_2$: C, 75.81; H, 7.11; N, 5.20. Found: C, 75.78; H, 7.54; N, 5.34. ^{1}H NMR (200 MHz, CD_3OD): δ = 7.14−7.42 (10H, m); 6.40−6.48 (1H, d); 4.08 (2H, s); 2.33 (3H, s). FT-IR (KBr): 3030, 2912, 2874, 2778, 2732, 2638, 2207, 1971, 1906, 1776, 1672, 1640, 1502, 1453, 1412, 1388, 1368, 1285, 1250, 1219, 1175, 1116, 1069, 1037, 982, 966, 920, 896, 884, 855, 836, 813, 752, 702, 620, 582, 543, 517, 493, 409 cm^{-1}.

8 *(3-MeCIN).* Mp 138 °C. Anal. Calcd for $C_{17}H_{19}NO_2$: C, 75.81; H, 7.11; N, 5.20. Found: C, 75.17; H, 7.64; N, 5.09. ^{1}H NMR (200 MHz, CD_3OD): δ = 7.11−7.42 (10H, m); 6.43−6.51 (1H, d); 4.09 (2H, s); 2.33 (3H, s). FT-IR (KBr): 3031, 2907, 2867, 2777,2633, 2341, 2198, 1973, 1853, 1786, 1641, 1604, 1582, 1529, 1453, 1425, 1390, 1371, 1292, 1263, 1219, 1171, 1156, 1091, 1069, 1002, 978, 922, 909, 894, 877, 817, 793, 752, 701, 683, 618, 591, 542, 526, 480, 433, 408 cm^{-1}.

9 *(2-MeCIN).* Mp 126 °C. Anal. Calcd for $C_{17}H_{19}NO_2$: C, 75.81; H, 7.11; N, 5.20. Found: C, 75.88; H, 7.52; N, 5.08. ^{1}H NMR (200 MHz, CD_3OD): δ = 7.17−7.78 (10H, m); 6.35−6.43 (1H, d); 4.09 (2H, s); 2.40 (3H, s). FT-IR (KBr): 3502, 3010, 2951, 2885, 2637, 2173, 1972, 1907, 1827, 1797, 1633, 1509, 1456, 1389,

1376, 1286, 1241, 1218, 1189, 1162, 1100, 1069, 1030, 982, 921, 882, 788, 771, 752, 731, 701, 600, 585, 557, 503, 477, 442 cm^{-1}.

10 *(4-NitCIN).* Mp 220 °C. Anal. Calcd for $C_{16}H_{16}N_2O_4$: C, 63.99; H, 5.37; N, 9.33. Found: C, 63.67; H, 5.66; N, 9.39. ^1H NMR (200 MHz, CD_3OD): δ = 8.20−8.24 (2H, d); 7.72−7.77 (2H, d); 7.40−7.48 (6H, m) 6.63−6.71 (1H, d); 4.10 (2H, s). FT-IR (KBr): 3271, 3032, 3012, 2891, 2742, 2685, 2606, 2170, 1919, 1781, 1644, 1582, 1551, 1514, 1454, 1414, 1378, 1341, 1287, 1245, 1214, 1177, 1156, 1108, 1065, 1029, 984, 966, 920, 892, 864, 846, 794, 756, 723, 700, 676, 645, 579, 541, 516, 485, 436 cm^{-1}.

11 *(3-NitCIN).* Mp 136 °C. Anal. Calcd for $C_{16}H_{16}N_2O_4$: C, 63.99; H, 5.37; N, 9.33. Found: C, 63.90; H, 5.49; N, 9.27. ^1H NMR (200 MHz, CD_3OD): δ = 7.56−8.35 (3H, m); 7.40−7.47 (7H, m); 6.50−6.67 (1H, m); 4.11 (2H, s). FT-IR (KBr): 3067, 3029, 2896, 2754, 2661, 2455, 2197, 1959, 1892, 1829, 1768, 1716, 1642, 1527, 1459, 1391, 1373, 1351, 1289, 1249, 1214, 1131, 1096, 1071, 1028, 973, 917, 876, 826, 810, 755, 720, 700, 673, 663, 619, 591, 553, 516, 493, 408 cm^{-1}.

12 *(2-NitCIN).* Mp 112 °C. Anal. Calcd for $C_{16}H_{16}N_2O_4$: C, 63.99; H, 5.37; N, 9.33. Found: C, 64.56; H, 5.58; N, 9.07. ^1H NMR (200 MHz, CD_3OD): δ = 7.43−7.96 (10H, m); 6.44−6.52 (1H, d); 4.11 (2H, s). FT-IR (KBr): 3059, 3035, 2855, 2140, 1872, 1790, 1746, 1657, 1634, 1604, 1557, 1521, 1471, 1461, 1440, 1388, 1375, 1342, 1308, 1295, 1213, 1195, 1161, 1136, 1073, 1044, 1030, 978, 930, 893, 875, 861, 835, 789, 756, 727, 704, 663, 619, 592, 579, 538, 489, 419 cm^{-1}.

13 *(CIN).* Mp 125 °C. Anal. Calcd for $C_{16}H_{17}NO_2$: C, 75.27; H, 6.71; N, 5.49. Found: C, 75.17; H, 6.96; N, 5.36. ^1H NMR (200 MHz, CD_3OD): δ = 7.32−7.53 (11H, m); 6.46−6.54 (1H, d); 4.10 (2H, s). FT-IR (KBr): 3286, 3047, 3028, 2969, 2851, 2761, 2663, 2633, 2505, 2192, 1967, 1887, 1813, 1764, 1639, 1576, 1529, 1496, 1449, 1374, 1325, 1286, 1249, 1200, 1175, 1156, 1139, 1102, 1071, 1027, 992, 965, 934, 882, 847, 778, 739, 718, 690, 619, 586, 535, 488, 462, 415 cm^{-1}.

14 *(HCIN).* Mp 96 °C. Anal. Calcd for $C_{16}H_{19}NO_2$: C, 74.68; H, 7.44; N, 5.44. Found: C, 74.28; H, 7.54; N, 5.51. ^1H NMR (200 MHz, CD_3OD): δ = 7.12−7.41 (10H, m); 4.05 (2H, s); 2.84−2.92 (2H, m); 2.40−2.48 (2H, m). FT-IR (KBr): 3501, 3028, 2999, 2959, 2923, 2785, 2741, 2647, 2527, 2214, 1959, 1886, 1825, 1766, 1634, 1544, 1496, 1452, 1439, 1390, 1347, 1312, 1297, 1286, 1217, 1199, 1174, 1156, 1073, 1029, 982, 953, 910, 860, 796, 770, 748, 697, 611, 580, 562, 488, 469, 404 cm^{-1}.

Single-Crystal X-ray diffraction. X-ray quality single crystals are grown in a slow evaporative condition at room temperature. The corresponding salts are dissolved in the crystallizing solvent with the aid of a few drops of MeOH. Crystals of **5**, **11**, and **13** are grown from *n*-heptane. Salt **2** is crystallized from cyclohexane. **6** is crystallized from acetonitrile. **7** is crystallized from isooctane. **8** and **9** are crystallized from ethyl acetate. Diffraction data are collected using Mo Kα (λ = 0.7107 Å) radiation on a Bruker AXS SMART APEX charge-coupled device diffractometer. All calculations were performed by using the software package of SMART APEX.

All structures are solved by direct methods and refined in a routine manner. In all cases, nonhydrogen atoms are treated anisotropically and hydrogen atoms attached to nitrogen are located on a difference Fourier map and refined. Whenever possible, the other hydrogen atoms are located on a difference Fourier map and refined. In rest of the cases, the hydrogen atoms are geometrically fixed. The crystallographic parameters are listed in Table 3. These data (CCDC 287025-287032) can also be obtained free of charge via www.cam.ac.uk/conts/retrieving.html (or from the Cambridge Crystallographic Data Center, 12 Union Road, Cambridge CB21EZ, UK..; fax, +44-1223-336033; e-mail, deposit@ccdc.cam.ac.uk).

Acknowledgment. Ministry of Environment and Forests, New Delhi, India, is thankfully acknowledged for financial support. D.T. thanks CSIR for a SRF fellowship.

Supporting Information Available: Hydrogen bonding parameters for the salts **2**, **5**−**9**, **11**, and **13** (Table S1) and XRPD comparison plots for the gelator salts **1**, **2**, **4**, **5**, **7**, **8**, and **11** (Figure S1) and nongelator salts **6** and **9** (Figure S2; PDF). This material is available free of charge via the Internet at http://pubs.acs.org.

CM0523586